Use of Artificial Neural Networks for Automatic Categorical Change Detection in Satellite Imagery

Conference Paper · November 2016

5 authors, including:

Patrick Doherty
Linköping University
208 PUBLICATIONS **2,736** CITATIONS

SEE PROFILE

Haroldo Fraga de Campos Velho
National Institute for Space Research, Brazil
366 PUBLICATIONS **1,590** CITATIONS

SEE PROFILE

Some of the authors of this publication are also working on these related projects:

Vibration-based damage identification using hybrid metaheuristics and a hierarchical approach View project

Data assimilation: using neural network for emulating NCEP-NOAA analysis (3D-Var method) View project

Use of Artificial Neural Networks for Automatic Categorical Change Detection in Satellite Imagery

José R. G. Braga [a1], Gianpaolo Conte [b], Patrick Doherty [b], Haroldo F. C. Velho [a]
and Elcio H. Shiguemori [c]

[a]National Institute for Space Research, São José dos Campos, SP, Brazil
[b]Linköpings Universitet, Linköping, Sweden
[c]Institute of Advanced Studies, São José dos Campos, SP, Brazil

Abstract

Change detection techniques based on post-classification comparison are used for monitoring the land-cover change using multi-temporal satellite imagery. A methodology for automatic land-cover change detection has been developed based on Artificial Neural Networks (ANNs) for multispectral image classification. The method developed is based on a classification step of the available images and a change detection step which makes use of the classified images. Three supervised learning ANNs are used: Multilayer Perceptron (MLP), Radial Basis Function (RBF) and Non-Extensible Radial Basis Function (NE-RBF). In addition, an unsupervised learning ANN technique called Self-Organized Map (SOM) is also used in this work. A texture analysis, using a gray-scale image, and a statistical analysis, using a RGB image, are applied to identify the inputs to the ANN. The texture analysis is done using Grey-Level Co-Occurrence Matrix (GLCM). The statistical analysis is done by calculating the average and standard deviation of a pixel with respect to its eight neighbor pixels in each of the bands composing the image, red (R band), green (G band), and blue (B band). Two images acquired from different periods of time (years 2003 and 2014) from Casalvieri (Frosinone province, Italy), have been employed to track the changes caused by the human action on the terrain. Our results demonstrate the potential of using ANNs for automatic land-cover change detection.

Keywords: Artificial Neural Network, Automatic Change Detection, Post-Classification Comparison Change Detection, Categorical Change Detection.

1. Introduction

Global environmental change is becoming a serious problem and a source of concern for the international community. Such alteration is linked to the

---

[1]E-mail Corresponding Author: jgarciabraga@gmail.com

local landscape changes and it may also produce ecosystem effects at some distance from the source [2]. The automatic land-cover change detection is an interesting and relevant image processing problem. It is beneficial in the process of understanding the impact of human actions on the environment [1].

Automatic landscape change detection is usually performed using two images of the same area taken at two different time points. It has been applied with success in many fields, such as: urban planning, analysis of population growth, monitoring of land use for agriculture and general environmental monitoring [5].

Due to the increasing environmental concerns, automatic change detection has become a topic of great interest within the scientific community. A large variety of automatic change detection methods have been developed [3, 4, 5]. The developed methods can be classified as:

- Change Mask Development (CMD): only changes and non-changes are detected. There is no information about the kind of change occurred.

- Categorical Change Extraction (CCE): the land-cover change is detected and categorized. Information about the type of changes is provided.

CMD does not identify what type of land-cover changes have occurred in the area of interest. However, CCE provides a complete categorization of the area of interest and it is more appropriate for the development of environmental monitoring techniques [2]. CCE can be divided into three categories: Change Vector Analysis, Direct Multidate Classification and Post-Classification Comparison.

The Change Vector Analysis method defines two vectors, where the first one stores information about the degree of change, while the second stores the type of change. Land-cover change detection is based on the analysis of these two vectors. This method is computationally expensive.

The Direct Multidate Classification method handles simultaneously the two remotely sensed images taken at different time points. This method performs an analysis of the combined data set of the two images in order to identify the changes. However, this method is suitable for remotely sensed images composed from several channels, for example hyperspectral images.

Post-Classification Comparison classifies each image and compares the color maps obtained from the classification process. The efficiency of the method depends on the accuracy of the classification algorithm chosen to generate the color maps.

Supervised and unsupervised ANNs approaches have both been used for classification of remotely sensed images [6]. The approaches based on ANNs have three main advantages when applied to image classification [4]: (1) ANNs do not require any assumptions on the input data distribution and they can learn from discontinuous and non-linear input data; (2) ANNs are self-adaptive and do not need prior knowledge of the input data; (3) ANNs can provide universal functional approximations.

The images used in this work are relative to an area placed in the Casalvieri municipality (Frosinone province, Italy). The RGB images were acquired at two different time points: the first image was acquired in 2003 and the second in 2014. The images were acquired from the Google Earth database.

For the classification step, three supervised ANNs are tested: Multilayer Perceptron (MLP), Radial Basis Function (RBF) and Non-Extensible Radial Basis Function (NE-RBF). Additionally, an unsupervised technique called Self-Organized Map (SOM) is also tested.

The ANNs input data are obtained by texture analysis using the Grey-Level Co-Occurrence Matrix (GLCM) and by calculating the average and standard deviation of a pixel. The results are evaluated in terms of performance of the classifier and correctness of the detected image changes

This paper is organized as follows: Section 2 describes the methodology. Section 3 presents the results obtained for image classification and change detection. Final considerations and conclusions are provided in Section 4.

2. Post-Classification Comparison Change Detection

Figure 1 depicts the proposed method for Post-Classification Comparison Change Detection.

2.1. Imagery Selection (A)

The input for the algorithm are two pre-registered images taken at different time points. The images are depicted in Figure 2. The oldest image was captured from the Quickbird satellite while the newest image comes from the Geoeye satellite. Both images have 1.65 meters/pixel resolution and provide RGB spectral information. The classes of interest in these images are: herb (transition between bare-soil and grass), concrete, grass, trees, bare-soil, and asphalt-road. A total of 5400 control points, from these classes, are selected to perform the evaluation of the ANNs-based classifier and for the change detection approach. Table 1 gives the distribution of control points among the classes of interest and the color information for identifying each class in
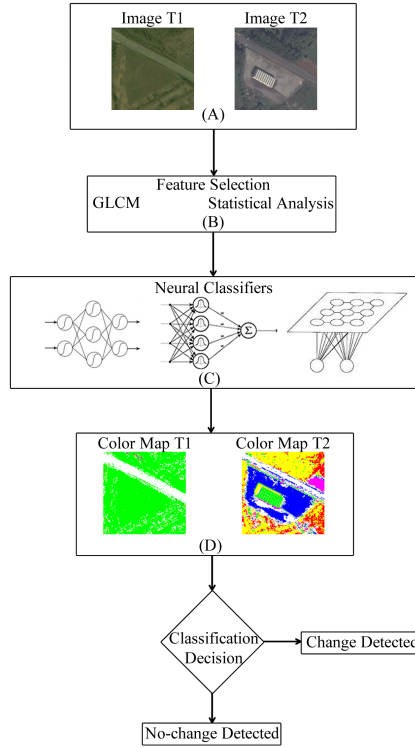
Figure 1: Change detection approach.

a color map.

The main changes on the ground were determined using the classes of interest over the images – see Table 1. The main transitions on the ground which contain the classes of interest are exhibited in Table 2. These changes in the land cover are used to evaluate the proposed method.

2.2. Feature Selection (B)

The feature selection used by the ANN classification method was performed by GLCM and statistical analysis. The GLCM is a two dimensional matrix used to calculate the texture attributes of an object in an image [11]. The texture attributes can describe objects defined as the variation of the gray level combination existing in an image. The variations of the gray level combination are computed along the direction with angles 0°, 45°, 90° and 135°. Thus for each texture attribute there are 4 values, one for each angle.

(A) Casalvieri 2003   (B) Casalvieri 2014

Figure 2: Registered remotely sensed images used in this work. In (A) the image captured by QuickBird in 2003. In (B) the image captured by Geoeye in 2014.

Table 1: In the table are reported the classes of interest, number of control points, number of elements chosen for the ANN training and identification color.

Classes of Interest	# Control Points(Pixels)	# for training(Pixels)	Color
Herb	2160	60	Green
Concrete	540	60	Blue
Grass	540	60	Red
Trees	540	60	Yellow
Asphalt Road	1080	60	Purple
Bare-Soil	540	60	Pink
Total	5700	360	

The most used texture attributes in the scientific community are:

$$\text{Energy} \quad = \quad \sum_{i=0}^{n-1}\sum_{j=0}^{m-1} P(i,j)^2$$

$$\text{Contrast} \quad = \quad \sum_{i=0}^{n-1}\sum_{j=0}^{m-1} P(i,j)\cdot(i-j)^2$$

$$\text{Homogeneity} \quad = \quad \sum_{i=0}^{n-1}\sum_{j=0}^{m-1} \frac{P(i,j)}{1+(i-j)^2}$$

where n is the image width, m is the image height, and $P(i,j)$ is the pixel value at position (i,j).

Table 2: Land-cover class transition used to evaluate the proposed method.

Class change	Amount (Pixels)
Herb → Concrete	540
Herb → Grass	540
Herb → Trees	540
Herb → Bare-soil	540
Asphalt-road → Asphalt-road	540
Total	2700

The statistical parameters (average μ and standard deviation σ) were computed by:

$$\mu = \sum_{i=0}^{n-1}\sum_{j=0}^{m-1} \frac{P(i,j)}{(n \cdot m)} \ ,$$

$$\sigma = \sqrt{\frac{\sum_{i=0}^{n-1}\sum_{j=0}^{m-1}(P(i,j) - \mu)^2}{(n \cdot m) - 1}} \ .$$

Statistical parameters and texture attributes were calculated based on a pixel and its eight neighbor pixels. The steps for the feature selection are: (i) 60 elements are randomly selected from the control points of each class of interest, (ii) μ and σ are computed for each band – this step provides 6 features for each element, (iii) images are converted into gray-level images, (iv) texture attributes are computed using the GLCM – this step produces 12 features for each element. Therefore, each input pattern is characterized by 18 features.

2.3. Neural Classifiers (C)

The ANN is a mathematical model, inspired by the human brain, designed to replicate brain behavior to solve particular problems. The ANN can be implemented in software or in hardware [7].

2.3.1. Multilayer Perceptron

The MLP is a feed-forward ANN widely used for solving linearly non-separable problems, and widely applied in classification problems [2]. Its architecture has three main features: (1) one input layer with non-computational

neurons, receiving the stimulus (data) from the environment; (2) one or more hidden layers composed by computational neurons; (3) one output layer with computational neurons. The computational neuron has a non linear activation function where different functions can be used.

The error back-propagation algorithm is the most used for the training phase [7]. The training phase consists of an iterative adjustment of the MLP weights, the connections between neurons. The generalized delta rule: $\Delta w(n+1) = \alpha \Delta w(n) + \eta \delta(n)y(n)$ is a well known strategy for updating the weights for this algorithm [7]. In the generalized delta rule α is the momentum value, η is the learning rate value, $\delta(n)$ is the gradient of the square difference between the ANN output and the target and finally $y(n)$ is the output produced by the MLP.

An additional research question involving the MLP is the determination of the best architecture to solve a specific problem. A common method for determining the MLP architecture is the trial and error approach. However, this issue can be addressed formulating the problem as one of optimization. Metaheuristics can be employed to solve optimization problems. The Multiple Particle Collision Algorithm (MPCA) has been applied to determine automatically the MLP architecture [10]. Applying the MPCA, the MLP architecture was identified with: 18 input neurons, 22 neurons in the hidden layer and 6 output neurons. The selected activation function chosen is the *hyperbolic tangent function*, $\alpha = 0.92$, and $\eta = 0.85$.

2.3.2. Radial Basis Function

The RBF ANN is able to model complex mapping and solve classification problems [7]. The RBF architecture consists of: (1) one input layer of non-computational neurons; (2) one, and just one, hidden layer of computational neurons implementing the radial basis activation function; (3) one output layer with computational neurons having a linear activation function. The output layer of a RBF performs a weighted sum of the hidden layer outputs.

The most used radial basis function is the Gaussian function:

$$G(d) = \left[\frac{1}{2\pi\sigma^2}\right]^{1/2} e^{-d^2/(2\sigma^2)} . \tag{1}$$

However, other radial basis functions can be implemented. The Tsallis distribution, derived in the context of non-extensive thermodynamics, can be used. A fundamental issue in the Tsallis generalized thermo-statistics is the non-extensivity parameter q [8].

The Tsallis distribution has been applied in the RBF and is named *non-extensible* RBF (NE-RBF) [9]. The expressions for the Tsallis distribution

is given by:

$$\text{For } q > 1: \ p_q(d) = \frac{1}{\sigma} \left(\frac{q-1}{\pi(3-q)} \right)^{\frac{1}{2}} \frac{\Gamma\left(\frac{1}{q-1}\right)}{\Gamma\left[\frac{3-q}{2(q-1)}\right]} \left[1 + \frac{q-1}{3-q} \left(\frac{d}{\sigma} \right)^2 \right]^{\frac{1}{1-q}} \quad (2)$$

$$\text{For } q < 1: \ p_q(d) = \frac{1}{\sigma} \left(\frac{1-q}{\pi(3-q)} \right)^{\frac{1}{2}} \frac{\Gamma\left(\frac{5-3q}{2-2q}\right)}{\Gamma\left(\frac{2-q}{1-q}\right)} \left[1 - \frac{1-q}{3-q} \left(\frac{d}{\sigma} \right)^2 \right]^{\frac{1}{1-q}} \quad (3)$$

For equations 1, 2, 3: $d = \|x - \nu\|$, where ν is the centroid position and x is the input data. $\sigma = d_{max}/\sqrt{2n}$, where d_{max} is the maximum distance among the centroids.

The RBF training consists of determining the parameters ν and also the weight values between the hidden layer and the output layer. The K-Means algorithm was used to determine the parameter ν. In addition, the solution of the linear system $W = A^{-1} \times Y_d$, was used for computing the weight matrix W, being A the matrix with the output values from the hidden layer and Y_d the matrix with the desired output values.

The RBF and the NE-RBF architectures were determined by varying the number of centroids (number of hidden neurons), and by varying the q parameter in the case of NE-RBF. The Gaussian RBF (or only RBF) architecture uses 18 input neurons, 60 centroids (or hidden layers), 6 output neurons. The NE-RBF architecture uses 18 input neurons, 60 centroids (or hidden layers), 6 output neurons, $q = 1.5$ – see Eq. (2).

2.3.3. Self-organizing Map

A SOM consists of a set of neurons organized on 2 dimensional grids, each neuron is a n-dimensional weight vector, where n is equal to the dimension of the input patterns [7]. In a SOM, adjacent neurons are connected and set the map topology which can be hexagonal or rectangular.

The SOM training algorithm modifies the values of the weight vector. The SOM training can be sequential or in batch. In the sequential training, the patterns are given to the neural network at each new input and the algorithm modifies the weight vectors. In the batch training, the data set is given to the SOM as whole (one epoch) and the adjustment in the weight vector is performed after each epoch.

In this work, the SOM neural network was implemented using sequential training. The SOM architecture was determined changing the amount of neurons in the grid and the topology. The final SOM configuration was

256 neurons distributed in a 16×16 grid with a hexagonal topology. The dimension of the input patterns is 18, equal to the number of features used to identify each pattern.

2.4. Classification Decision

The classification decision is performed comparing the color maps produced from the image classification by the ANNs. The ANN classification generates color maps, following the color information expressed in Table 1. The first step is then to classify the two available images. The classification results can be visualized in the form of two color maps, one for each classified image, following the color scheme presented in Table 1. The system detects the land-cover change by comparing the occurrence of color change in both color maps.

3. Results

For the evaluation of the results 5400 control points were used. Of these total control points, 2160 are from herb and 540 are from asphalt road. These points were selected from the Casalvieri 2003 image. The other 2700 control points are equally distributed in the classes concrete, grass, trees, asphalt road and bare-soil. These control points were taken from the Casalvieri 2014 image.

The evaluation of the method presented consists in assessing the performance of the proposed classifier and in the analysis of the change detection results.

In regard to the classifier, the evaluation was conducted using 5400 control points. A confusion matrix was used as a metric to evaluate the results.

In regard to the evaluation of the change detection results, 2700 class changes were used. For this purpose three different metrics have been used:

1. Positive Reliability for Change (PRC, [%]), $PRC = \frac{TP_c}{TP_c + FN_c} \cdot 100$, where TP_c (True Positive for Change) is the amount of changes correctly detected and FN_c (False Negative for Change) is the amount of changes detected incorrectly;

2. Positive Reliability for Non-change (PRN, [%]), $PRN = \frac{TP_n}{TP_n + FN_n} \cdot 100$, where TP_n (True Positive for Non-change) is the amount of non-changes correctly detected and FN_n (False Negative for Non-change) is the amount of non-changes incorrectly detected;

3. Total Success Rate (TSR, [%]), $TSR = \frac{PRC + PRN}{2}$.

Tables 3, 4, 5, and 6 show the confusion matrices for the classification results using SOM, MLP, RBF, and NE-RBF, respectively. The bottom-right element of the matrices represents a global performance value of the adopted classifier.

Table 3: Confusion matrix for the control point classification using SOM.

	Predict						
	Herb	Concrete	Grass	Trees	Asphalt road	Bare-soil	Total
Herb	1970	0	0	36	154	0	91.2%
Concrete	0	502	1	1	36	0	93.0%
Grass	0	0	520	17	3	0	96.3%
Trees	1	0	9	515	15	0	95.4%
Asphalt-road	56	32	16	6	956	14	88.5%
Bare-soil	0	0	2	2	2	534	98.9%
Total	97.2%	94.0%	94.9%	89.3%	82.0%	97.4%	92.5%

Table 4: Confusion matrix for the control point classification using MLP.

	Predict						
	Herb	Concrete	Grass	Trees	Asphalt-road	Bare-soil	Total
Herb	2067	0	7	1	83	2	95.7%
Concrete	0	503	0	0	34	3	93.1%
Grass	0	0	512	14	14	0	94.8%
Trees	0	1	9	530	0	0	98.1%
Asphalt-road	46	64	8	0	942	20	87.2%
Bare-soil	0	3	0	1	3	533	98.7%
Total	97.8%	88.1%	95.5%	97.1%	87.5%	95.5%	94.2%

Table 5: Confusion matrix for the control point classification using RBF.

	Predict						
	Herb	Concrete	Grass	Trees	Asphalt-road	Bare-soil	Total
Herb	2071	1	0	11	77	0	95.9%
Concrete	0	457	0	0	82	1	84.6%
Grass	0	0	531	6	3	0	98.3%
Trees	1	6	13	508	12	0	94.1%
Asphalt-road	32	10	0	4	1014	20	93.9%
Bare-soil	0	0	0	1	0	539	99.8%
Total	98.4%	96.4%	97.6%	95.8%	85.4%	96.3%	94.8%

Table 6: Confusion matrix for the control point classification using NE-RBF.

	Predict						
	Herb	Concrete	Grass	Trees	Asphalt-road	Bare-soil	Total
Herb	2063	0	0	0	96	1	95.5%
Concrete	0	453	0	0	87	0	83.9%
Grass	0	0	531	6	3	0	98.3%
Trees	14	0	15	504	7	0	93.3%
Asphalt-road	28	10	0	6	1018	18	94.3%
Bare-soil	0	0	0	1	0	539	99.8%
Total	98.0%	97.8%	97.3%	97.5%	84.1%	96.6%	94.6%

Table 7 presents the results of the three evaluation metrics (PRC, PRN, and TSR) used to evaluate the ANNs with respect to change detection.

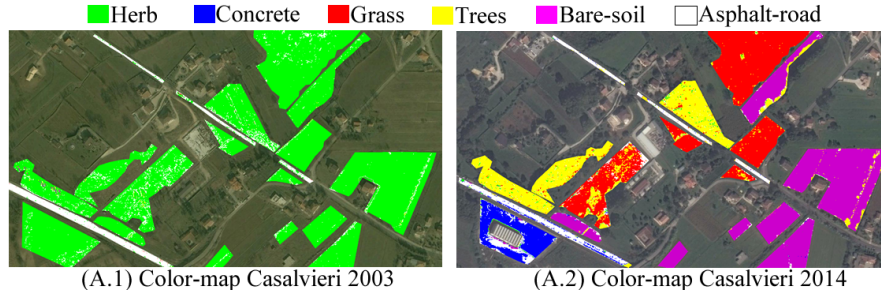**Table 7:** Value of metrics PRC, PRN and TSR used to evaluate the ANNs with respect to change detection.

|	PRC	PRN	TSR
SOM	87.45%	80.74%	84.10%
MLP	91.99%	78.15%	85.07%
RBF	90.23%	91.48%	90.86%
NE-RBF	89.49%	92.22%	90.86%

4. Conclusions

Figure 3 depicts the result of the classification performed by RBF in the two satellite images from Casalvieri at the two time points.

Figure 4 exhibits the result of change detection by comparing the color maps. The green points are the correct changes detected and the red points are the incorrect changes detected.

The algorithms and methodology proposed in this paper show encouraging results for automatic land-cover change detection using the Post-Classification Comparison. The experimental results show that ANNs are suitable to treat the classification problem, considering unsupervised and supervised strategies. This can be observed from the index obtained from the confusion matrix, above of 92.0% for all neural classifiers. The correctness of the change detection depends greatly on the performance of the classifier. The RBF and NE-RBF give a TSR of 90.86%. Those results show that all ANNs used in this research, mainly RBF and NE-RBF, are

Herb ■ **Concrete** ■ **Grass** ■ **Trees** ■ **Bare-soil** □ **Asphalt-road**

(A.1) Color-map Casalvieri 2003   (A.2) Color-map Casalvieri 2014

Figure 3: In (A.1) the Casalvieri 2003 color map from the classification results obtained by RBF. In (A.2) the Casalvieri 2014 color map from the classification results obtained by RBF.

■ **Correct change detected**   ■ **Incorrect change detected**

(A.1) Casalvieri 2003   (A.2) Casalvieri 2014
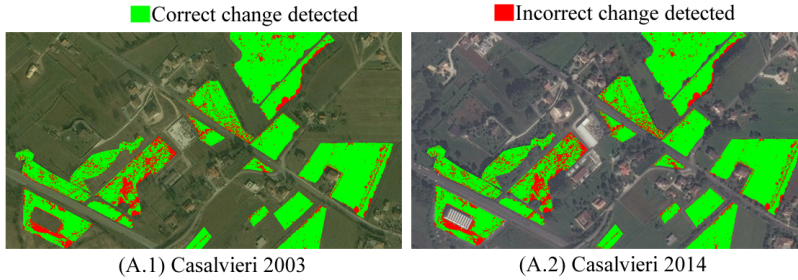
Figure 4: The green points are the correct changes detected and the red points are the incorrect changes detected.

suitable for land-cover change detection by Post-Classification Comparison. The NE-RB is a new approach for supervised ANN. Our results extend the application of the NE-RBF neural network.

References

[1] Neagoe, V.E., Neghina, M., Datcu,M. Neural Network Techniques for Automated Land-Cover Change Detection in Multispectral Satellite

Time Series Imagery, International Journal of Mathematical Models and Methods in Applied Sciences, Vol. 6, No. 1, 2012, pp. 130-139.

[2] Dai, X.L., Khorram, S. Remotely Sensed Change Detection Based on Artificial Neural Network, Photogrammetric Engieering and Remote Sensing, Vol. 65, No. 10, 1999, pp. 1187-1194.

[3] Lu, D., Mausel, P., Brondízio, E., Moran E. Change Detection Techniques, International Journal of Remote Sensing, Vol. 25, No. 12, 2010, pp. 2365-2407.

[4] Pacifici, F., Del Frate, F., Solimini, C., Emery, W.J. An Innovative Neural-Net Method to Detect Temporal Changes in High-Resolution Optical Satellite Imagery, IEEE Transactions on Geoscience and Remote Sensing, Vol. 45, No. 9, 2007, pp. 2940-2952.

[5] Mota, R.L.M., Ramos, A.C.B., Shiguemori, E.H. Application of Self-Organizing Maps at Change Detection in Amazon Forest, International Conference on Information Technology: New Generations, Vol. 1, No. 11, 2014, pp. 371-376.

[6] Silva, W., Habermann, M., Shiguemori, E.H., Andrade, L. L., Castro, R. M. Multispectral Image Classification using Multilayer Perceptron and Principal Components Analysis, 1st BRICS Countries Congress on Computational Intelligence, Porto de Galinhas, 2013.

[7] Haykin, S. Redes neurais princípios e práticas, Bookman, 2001, pp 900.

[8] Tsallis, C., Possible generalization of Boltzmann-Gibbs statistics. Journal of Statistical Physics, Vol. 52, No. 1-2, 1988, pp. 479-487.

[9] Shiguemori, E. H. Temperature and Moisture Profile Retrieval from Satellite Data: Approach by Artificial Neural Networks and Hardware Implementation, PhD Thesis in Applied Computing, INPE-Brazil, 2007. (In Portuguese)

[10] Anochi, J., Campos Velho, H.F., Furtado, H.C.M., Luz, E. Self-configuring Two Types Neural Networks by MPCA 2nd International Symposium on Uncertainty Quantification and Stochastic Modeling, 2014.

[11] Haralick, R., Shanmugan, K., Dinstein, I. Textural Features for Image Classification. IEEE Transactions on Systems Man and Cybernetics, Vol. 3, 1973, pp. 610-621.